Sled tests using the THOR-NT device and post mortem human surrogates in frontal impacts

Narayan Yoganandan, Frank Pintar, Jason Moore,
Michael Schlick, John Humm, James Rinaldi, Dennis J. Maiman

Abstract The purpose of this study was to compare motions and loads between the Test device for Human Occupant Restraint (THOR) and post mortem human surrogates (PMHS) in frontal impact sled tests with a focus on head-neck complex. The overall focus of the project was to evaluate the biofidelity characteristics and derivation of THOR-specific injury criteria. Experiments were conducted at low, medium, and high velocities using custom-designed seat. Upper and lower neck forces and moments were determined from load cell signals and locations. Based on motion and load variables (x- and z-displacement profiles; maximum x- and z-displacements; timing of motion vectors; upper and lower neck axial and shear forces and bending moments), it was concluded that the repeatability performance of the THOR dummy is acceptable at all tested velocities. This type of evaluation using many variables adds confidence to the evaluation/use of any device for a range of external frontal impact insults. Judging by similarities in the upper and lower neck loading profiles and maxima, it was further concluded that the THOR mimics the human head-neck responses well at all velocities. The THOR can be used effectively in frontal impact crashworthiness tests regardless of the change in velocity.

Keywords THOR, upper neck loads, lower neck loads, injuries, frontal impact, biomechanics, kinematics

I. INTRODUCTION

Anthropomorphic test devices, commonly termed crash test dummies or dummies, are routinely used in crashworthiness studies for improving road safety. These include simulated impacts such as sled tests and pendulum experiments, and full-scale vehicle tests such as those used in compliance and New Car Assessment Program (NCAP) tests around the world. Dummies are not omnidirectional. In other words, different dummies are used under different modes of impact. The Hybrid III dummy was developed to advance crashworthiness of motor vehicles in the United States for frontal impact applications. This dummy has been used in rollover testing, although it was developed only for frontal crashes. The side impact dummy, termed SID, was originally designed and developed in the 1980s to advance side impact crashworthiness. The European Side Impact dummy, ES2-re in the United States and ES2 in Europe, is currently used for certification for lateral impact crashworthiness tests [1].

From a frontal impact perspective, regardless of the use or the availability of different types of the three-point belt systems, the Hybrid III dummy is being used since the 1970s and around the world for frontal impact evaluations. This dummy is the specified physical device for evaluating frontal impact crashworthiness of vehicles in the United States and in other countries. The head-neck design of the dummy is based on performance guidelines developed before 1973. Biomechanical data under sagittal plane loading were obtained from sled tests consisting of a rigid seat, and a lap and criss-cross type shoulder belts were used as the restraint system. Data were plotted as the variation of the sagittal bending moment about the occipital condyles with respect to the head angle relative to the human torso. The Hybrid III dummy head-neck response was generally within the moment-angle human corridor under the flexion-extension. Since the design of this dummy, considerable advancements have been made in impact biomechanics studies using PMHS and other models. New research data and changes in vehicle design approaches and public awareness for safety have resulted in the development of newer test devices.

Narayan Yoganandan PhD, Professor of Neurosurgery and Orthopaedic Surgery; Chair, Biomed Eng.; Department of Neurosurgery, Medical College of Wisconsin, Milwaukee, 53226, WI, USA (phone: 414-384-3453, fax: 414-384-3493, e-mail: yoga@mcw.edu). Frank A. Pintar, PhD, Professor of Neurosurgery; Jason Moore, MS, Michael Schlick, MS, and John Humm, MS; Research Engineers; James Rinaldi, DC, Research Scientist, and Dennis J. Maiman, MD, PhD, Chair, Department of Neurosurgery, Medical College of Wisconsin, Milwaukee, 53226, WI, USA.

The Test Device for Human Occupant Restraint (THOR) was developed from a project sponsored by the National Highway Traffic Safety Administration of the United States Department of Transportation. This device was meant to be superior to the Hybrid III dummy. The device was designed using more recent biomechanical data, including responses from human volunteer tests performed at the Naval Biodynamics Laboratory, New Orleans, LA; and tests conducted at the Medical College of Wisconsin using post mortem human surrogates [2, 3]. The mechanical response of this dummy also falls within the human-based occipital condylar moment-angle corridors, described earlier. The dummy is more compliant in the axial (compressive response) mode than its predecessor. The axial response of the THOR better mimics the human response than the Hybrid II dummy [2, 4]. The THOR has two load cells in the neck: the upper one is at the junction of the head and neck and the lower one is at the transition between the neck and thorax. Thus, it is possible to record the forces at the ends and evaluate the biomechanics of the upper and lower cervical spines. Studies have been conducted to evaluate the performance of the dummy using mini-sled pendulum and full-scale sled equipment [3]. However, comparative evaluations of the upper and lower head-neck responses with matched-pair tests using PMHS experiments are necessary to better characterize biofidelity. The objective of the present study is to evaluate the dummy repeatability using kinematics and upper and lower neck loads, and compare its kinetic responses with PMHS at three different changes in velocities using sled tests from our laboratory.

II. METHODS

A generic sled buck was used to accommodate varying anthropometries and control occupant pre-positioning. The buck consisted of a rigid seat, head restraint and knee bolster. Its seat pan was oriented at an angle of 75 degrees with respect to the vertical. The seat back was oriented at an angle of 25 degrees with respect to the vertical. The head restraint was adjustable along the horizontal (x) and vertical (z) axes to maintain the pre-impact head-neck position. The head restraint was in contact with the back of the head. The knee bolster was adjustable along these directions. It was angled parallel to the lower limbs. The knee bolster was padded with paper honeycomb padding. The head Frankfort plane of the THOR-NT, termed THOR, was aligned parallel to the horizontal plane. To simulate normal posture, the knee bolster was adjusted such that an initial gap of 25 mm was allowed between the lower limb of the THOR and the paper honeycomb padding. A generic three-point belt with an adjustable D-ring was used. The belt was fixed along the x-axis, while it was capable of adjusting in the z-axis so that anthropometry differences could be incorporated to achieve similar pre-positioning between different surrogates. The lower anchor positions of the three-point belt were typical of a mid-size sedan vehicle.

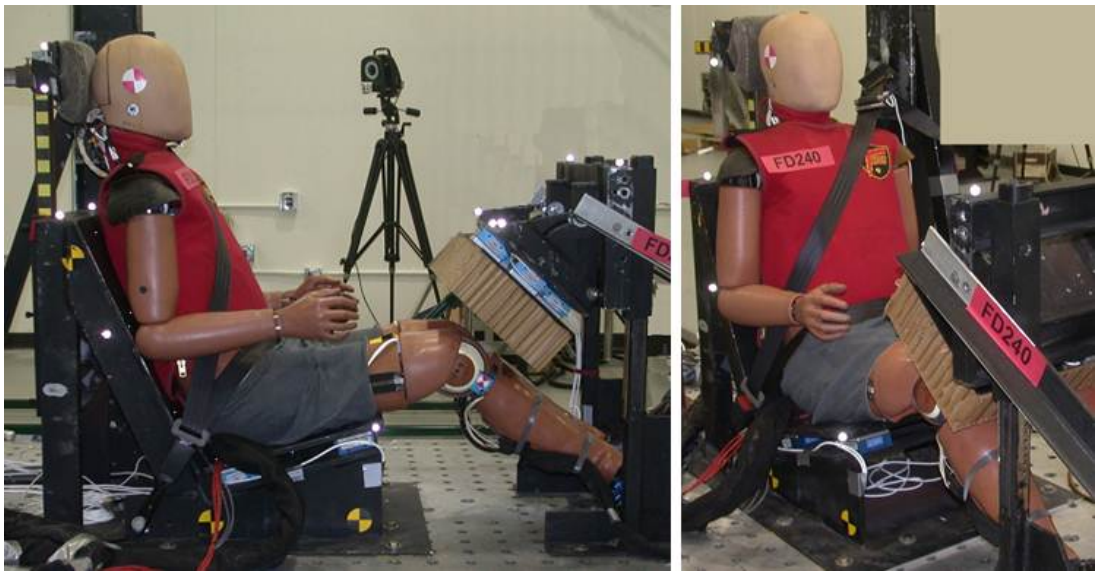

Figure 1: Photograph showing the THOR seated in the generic frontal buck. Left shows the side view. Right shows the frontal oblique view. See text for details.

A uniaxial accelerometer (Endevco model 7264C-2000, Fairfield, NJ) was secured to the sled equipment to record the input loading pulse. The change in velocity was determined from this signal. The upper and lower neck load cells were used to record forces and moments at the ends of the neck. Measured load cell data were transformed to obtain metrics at the upper and lower necks, equivalent to locations of the mid-line of the occipital condyles or the head-neck junction and the cervico-thoracic spinal junction, corresponding to the first thoracic vertebra in the human. Lever arms based on design drawings and load cell specifications were used to transform the recorded forces and moment signals. The upper neck load cell of the dummy is in-line with the occipital condyles horizontally, and vertically, it is situated inferiorly with respect to the occipital condyles. For the anatomic T1 location, the lower neck load cell is at the appropriate location in the dummy. Two uniaxial load cells (Denton Inc., Rochester Hills, MI) were used on the lap and shoulder belts to record restraint system forces. Three different changes in velocities were used: 3.6, 6.9 and 15.8 m/s representing low, medium, and high change in velocities. Repeated tests were done at each change in velocity. All signals were gathered from dummy sensors at 12,500 Hz, and data were processed and filtered according to the Society of Automotive Engineers Specifications [5].

The right-handed Cartesian coordinate system of reference was used according to SAE specifications. The posterior-to-anterior axis was positive along the x, left-to-right axis was positive along the y-, and superior-to-inferior direction was positive along the z-axes. Kinematic data were gathered using a digital motion tracking system, described later. For load data, the axial force was associated with the z-axis, and tensile force was positive. The bending moment was represented by the sagittal moment in the x-z plane, and forward flexion moment was positive. Forces and moments at the upper and lower necks were filtered at class 600 and sled accelerations were filtered at class 60. Forces and moments were evaluated for morphologies, peak magnitudes, and variations with respect to PMHS data, described below.

Tests with PMHS conducted under similar experimental conditions included positioning the biological surrogate on the same custom-designed seat, testing at three velocities, and use of appropriate sensor to compute forces and moments at the occipital condyles and cervico-thoracic junction; details are provided [6]. Briefly, a custom-designed pyramid-shaped nine accelerometer package (PNAP) was secured to the skull [7]. The package consisted of three linear accelerometers along the three orthogonal axes at the vertex and two linear accelerometers at each of the three legs of the pyramid. An instrumentation mount was attached to the spine of the first thoracic vertebra via bilateral pedicle screws from which a tri-axial accelerometer was attached.

The specimens were prepared with retro-reflective targets to obtain kinematics optically. A set of no less than three non-collinear targets were secured to the first thoracic vertebra using the accelerometer mount. A similar array of targets was attached to the outer periphery of the head of the specimen. Data from the retro-reflective targets were gathered using an optoelectronic stereo-photogrammetric 20-camera motion tracking system (Vicon, Oxford, UK). The cameras tracked positions of the retro-reflective targets in a calibrated three-dimensional space at 1000 frames/sec. A high-speed video camera captured the overall head-neck kinematics in the sagittal plane.

Linear and angular accelerations of the head were computed using the recorded set of nine accelerations from the PNAP and head geometry. Forces and moments at the upper neck were computed using head accelerations, inertial properties of each specimen, and dynamic equations of equilibrium [6-9]. The forces and moments at the lower neck were computed by assuming the neck to be the mass-less connecting link to the head and using the following methods.

The positions of the anatomic fiducials of the first thoracic vertebrae relative to its retro-reflective targets were determined using a coordinate measuring machine, a device used to measure the physical geometrical characteristics of an object. The equipment used a mechanical contact arm to obtain the coordinates of a desired location on the PMHS using joint angles and segment lengths (Faro-arm Inc., Lake Mary, FL). The origin of the first thoracic vertebra was defined at the posterior superior edge of the body. These data were included in the three dimensional kinematic model of the test to determine the position and orientation matrix of the

head with respect to the thoracic vertebra. The loads at the upper neck were transformed to the thoracic coordinate system using the matrix to compute forces and moments at the lower neck.

The trajectories of the center of gravity of the head (x-z displacements) with respect to the sled were determined. The position of the anatomic fiducials of the Frankfort plane, i.e., left and right auditory meatus and left and right infra-orbital notches, and bilateral sagittal plane projections of the head center of gravity relative to the head targets, were determined using data obtained from the coordinate measuring device. Similar measurements were made using the device to define the location of the sled coordinate system relative to the markers on the sled.

Data were transformed into a local target coordinate system and incorporated into a three dimensional kinematic model to determine the position and orientation of the head anatomy with respect to the sled. Trajectories were standardized so that the position of the head center of gravity coincided with the origin in all tests and at all velocities. Motion and loading results along with repeatability performance of the dummy are presented below.

III. RESULTS

Results from repeated tests for the THOR in terms of the kinematics expressed as head-neck trajectories and loads expressed as forces and moments at the upper and lower necks are presented. At low, medium, and high velocities, the maximum displacement along the x-axis was 182, 293, and 395 mm; and the maximum displacement along the z-axis was 104, 274, and 414 mm, respectively. These results are depicted in figure 2. As can be seen, the curve morphologies are similar at all velocities for displacements along both axes. Increasing velocity tests responded with increasing displacements, and good repeatability can be observed at all energy inputs.

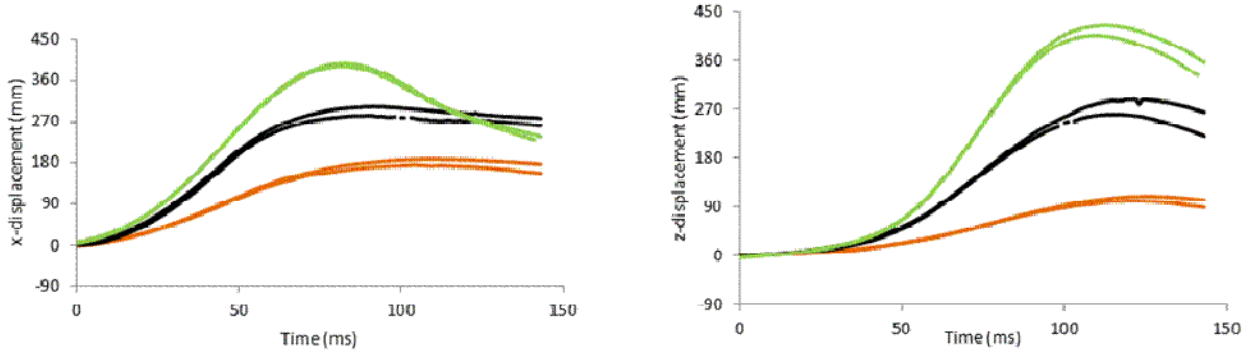

Figure 2: Kinematic repeatability responses of the THOR head along the horizontal and vertical axes, shown as x plot on the left and z plot on the right at the three velocities. Two plots shown for each velocity represent duplicate tests in each illustration. Low velocity responses are shown in brown, medium velocity responses are in black, and high velocity responses are in green color.

Additional results from repeated tests depicting the shear forces at the upper and lower necks are shown in figure 3, axial forces are shown in figure 4 and sagittal bending moments are shown in figure 5. As can be seen, all responses, like the kinematic responses in the z-x plane show good repeatability at all velocities and for all the six loading parameters in the THOR. As expected the bending moments are amplified at the lower neck in all tests, while the axial and shear forces do not respond with similar magnifications. Reasons are discussed in the next section.

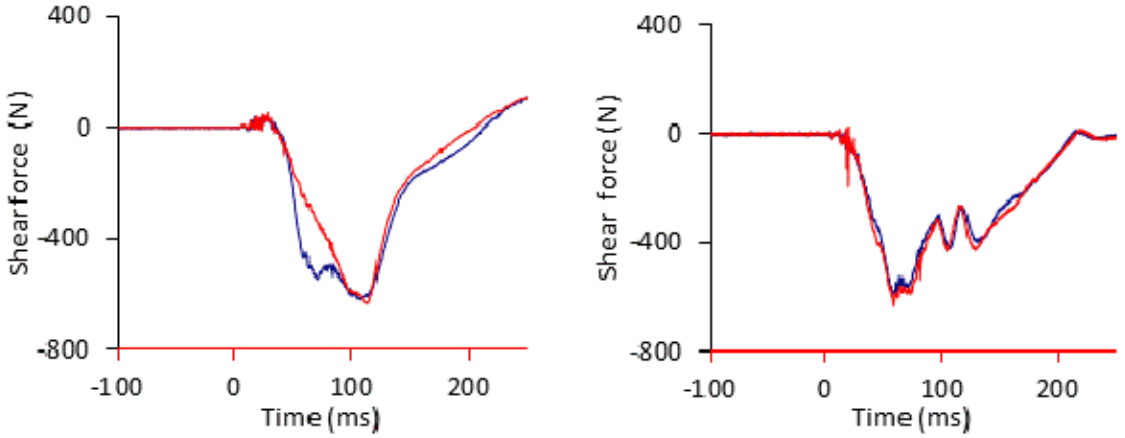

Figure 3: Kinetic repeatability responses of the THOR. Shown are the shear forces at the upper neck (left set of curves) and lower neck (right set of curves). All data correspond to the medium velocity tests. Two plots shown for each velocity represent duplicate tests in each illustration.

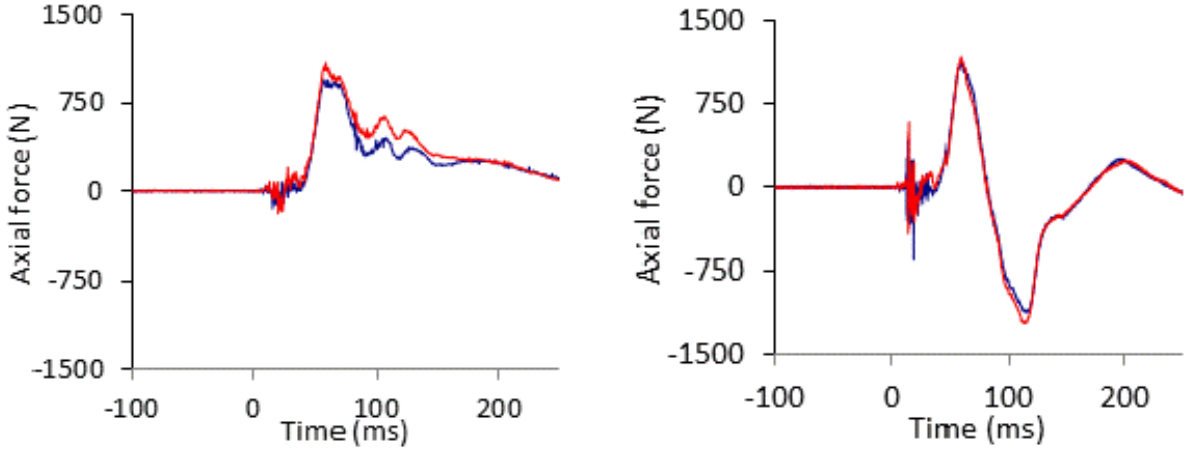

Figure 4: Kinetic repeatability responses of the THOR. Shown are the axial forces at the upper neck (left set of curves) and lower neck (right set of curves). All data correspond to the medium velocity tests. Two plots shown for each velocity represent duplicate tests in each illustration.

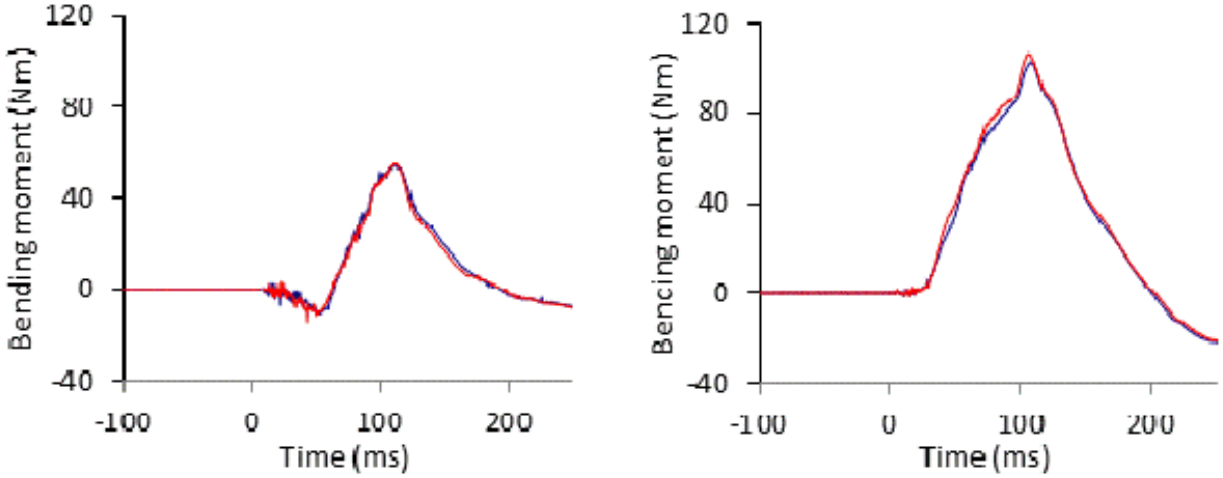

Figure 5: Kinetic repeatability responses of the THOR. Shown are the bending moment responses at the upper neck (left set of curves) and lower neck (right set of curves). All data correspond to the medium velocity tests. Two plots shown for each velocity represent duplicate tests in each illustration.

Head trajectories represented as corridors (obtained by plotting the range of data from all tests) at the three velocities are shown in figure 6. These trajectories are compared with trajectories from PMHS tests.

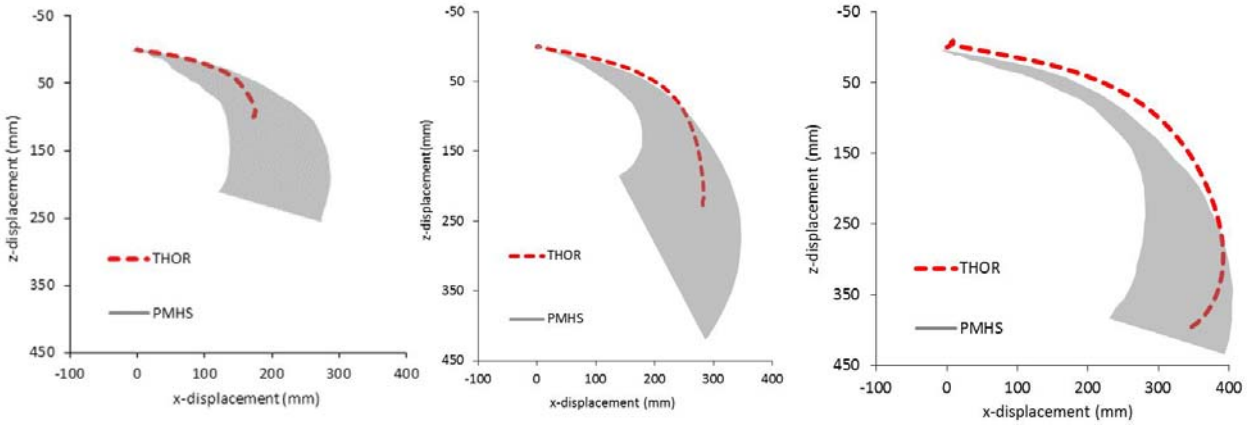

Figure 6: Responses of the THOR trajectories compared with PMHS response corridors at three energy inputs: from left to right corresponding to low, medium and high changes in velocity. Corridors are shown as blue shaded areas. THOR responses are shown as dashed curves in each plot.

In general, head trajectories remained within the PMHS corridor at all velocities, although the responses shifted towards the flexible end (right side) of the PMHS kinematics. The following approach was used to determine the deviations in the dummy responses from PMHS responses based on peak magnitudes of displacements in the sagittal plane. From the trajectory curve, as shown in an example in figure 7, the mean and one standard deviation limit in the peak PMHS responses along the x- and z-directions were obtained.

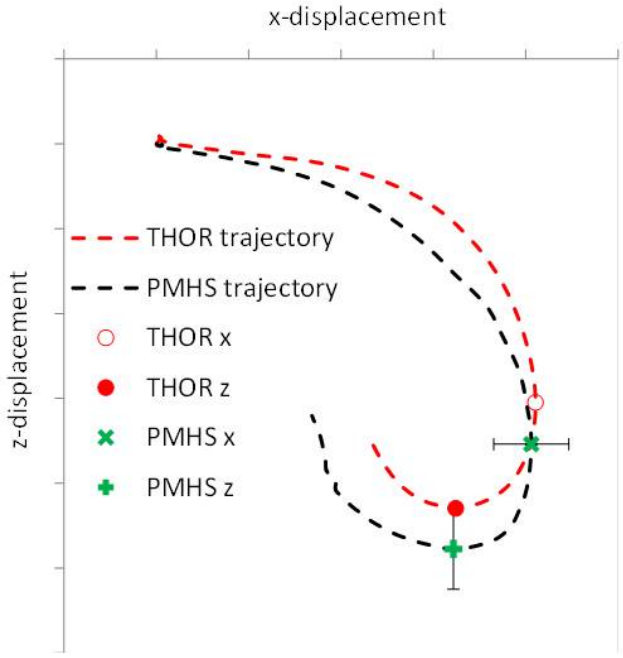

Figure 7: Generic trajectory (black dashed lines) showing the peak x- and z-data points along with plus/minus one standard deviation for PMHS displacements. Note the peak x- and z-motions occur at different points on the trajectory. Generic trajectories for the THOR are also shown (red dashed lines). Peak motion components are compared with the THOR responses at each velocity in figure 8.

This process yielded two datasets corresponding to the peak x- and z-displacement for each PMHS surrogate at each velocity. For the three velocities, six discrete peak magnitude-based head displacements (mean and one standard deviation) were obtained. The mean peak x- and z-displacement data for the THOR were plotted along with the mean and one standard deviation data for the PMHS for each velocity. If dummy displacements were within the PMHS mean and one standard deviation limit, the response was considered more biofidelic than if it was outside one standard deviation of the PMHS data. Low, medium and high velocity-specific peak displacement plots of the THOR were compared with PMHS mean and one standard deviation data. These plots are shown in figure 8.

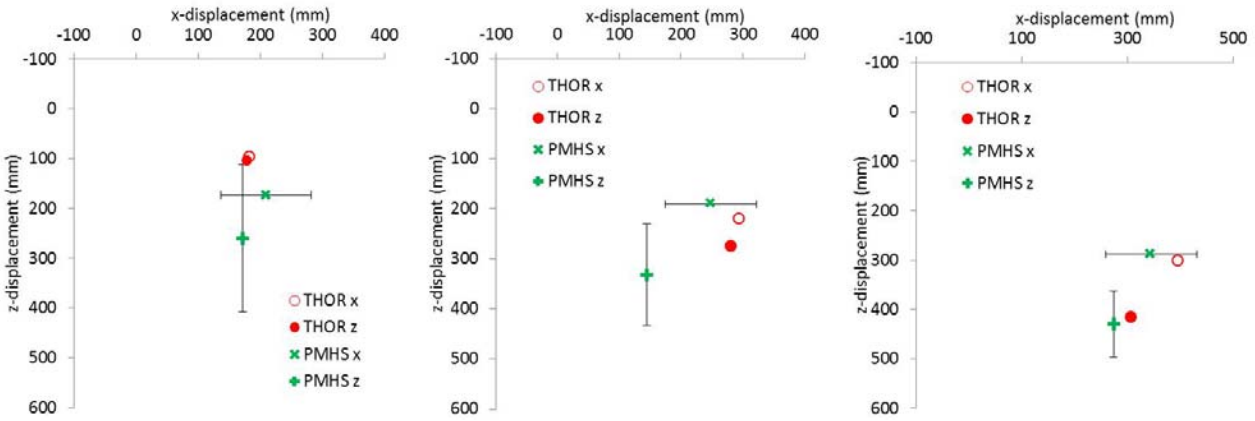

Figure 8: Deviations in the THOR displacements from PMHS data for the low (left), medium (middle) and high (right) velocity tests. Peak x- and z- displacements are shown in red for THOR. Mean PMHS data are shown in green and plus/minus one standard deviation lines are shown in black color.

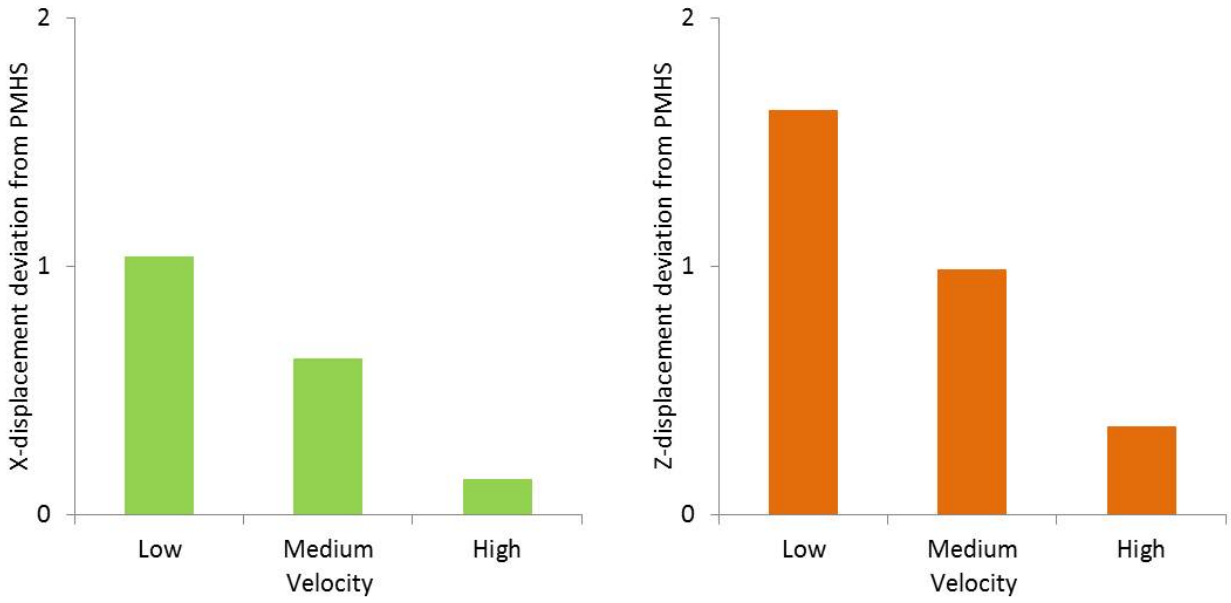

Figure 9: Deviation of the THOR response from PMHS for the time of attainment at the three velocities. The ordinate corresponds to the number of standard deviations away from the mean PMHS value for the x-displacement time (left) and z-displacement time (right).

Table 1: THOR biofidelity as determined by whether the peak magnitude and time of attainment of the peak displacement are within or outside one standard deviation based on PMHS data.

Velocity	x-displacement	z-displacement
Low	Yes	No
Medium	Yes	Yes
High	Yes	Yes

An examination of the times of attainments from the experiments indicated that the THOR reached its maximum x- and z-displacements earlier than the biological surrogate. This was true at all velocities (exception, x-displacement at the high velocity). Figure 10 shows these data (standard deviations are included for PMHS experiments) for the three velocities.

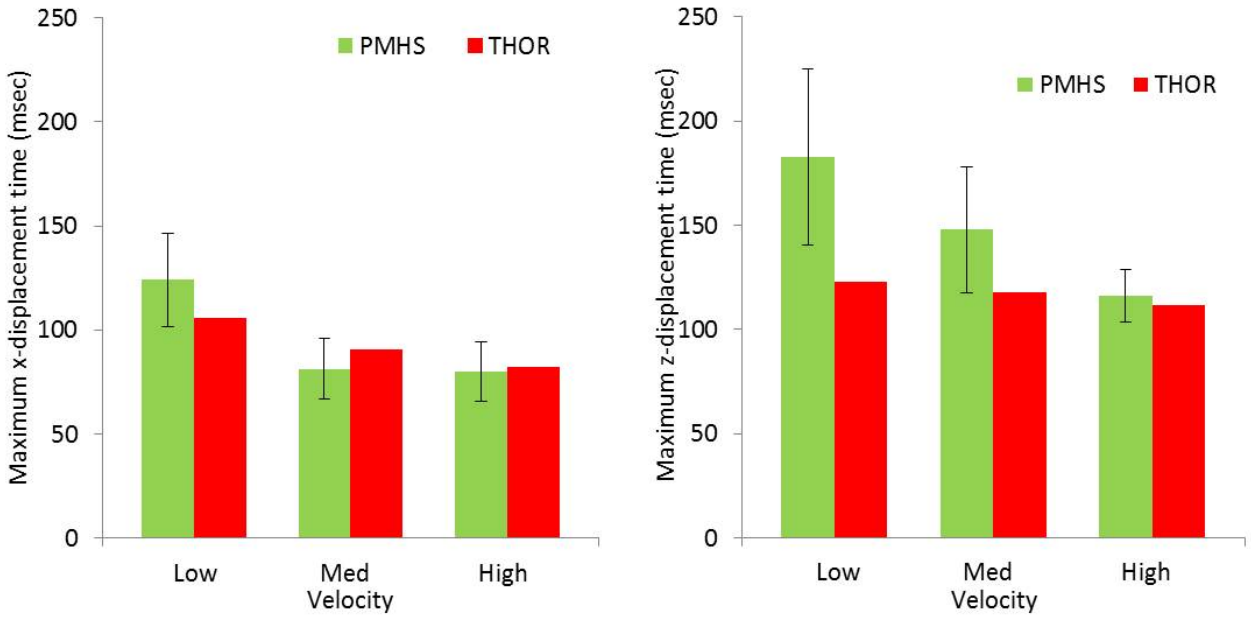

Figure 10: Times of attainment of peak x- (left) and z-displacements (right) for the PMHS and THOR. Data are drawn to the same scale as the z-displacements. PMHS data are shown as mean and plus/minus on standard deviation at each velocity and for both components.

At the upper neck for the THOR, maximum axial forces were 353, 1019 and 2727 N; shear forces were 285, 626 and 842 N; and bending moments were 23, 56 and 72 Nm, at the low, medium, and high velocities. At the lower neck, maximum axial forces were 302, 1155 and 2132 N; shear forces were 285, 612 and 758 N; and bending moments were 49, 104 and 134 Nm, at the low, medium, and high velocities, respectively. These responses are compared with PMHS data.

Figure 11 shows the mean maximum axial and shear forces from PMHS and THOR tests at all velocities at the upper and lower necks. Figure 12 shows the bending moment data from PMHS and THOR tests at all velocities at the upper and lower necks.

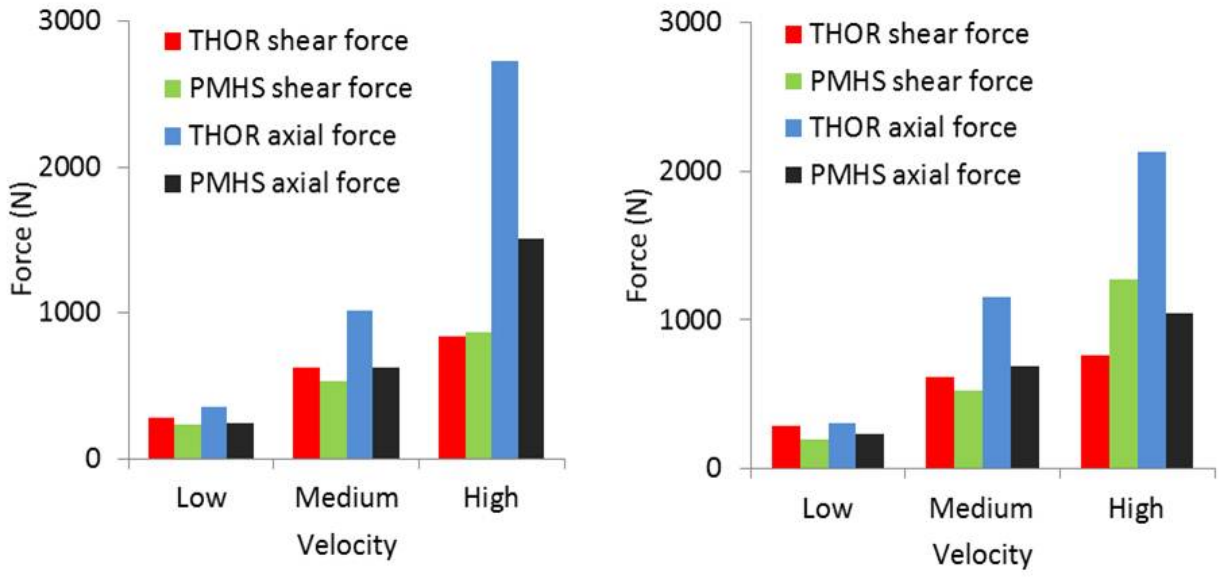

Figure 11: Comparison of maximum upper (left) and lower (right) shear and axial forces in PMHS and THOR

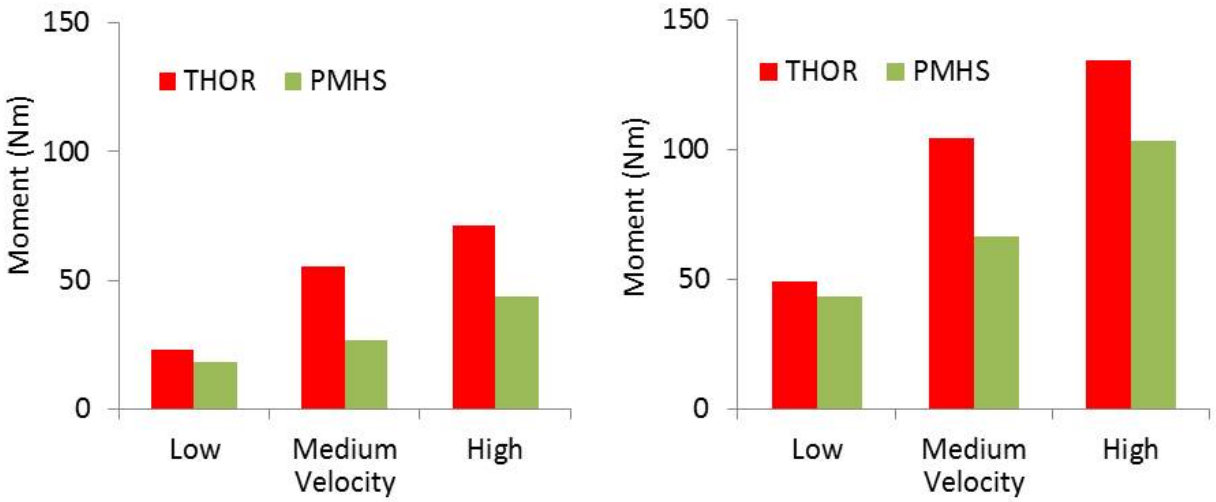

Figure 12: Comparison of maximum upper (left) and lower (right) bending moments in PMHS and THOR

IV. DISCUSSION

As described in the introductory paragraphs of this manuscript, the aim of the present study was to evaluate the response of the THOR in simulated frontal impacts using sled equipment. The objective was achieved by evaluating biomechanical variables including motions and loads at the ends of the neck. Based on motion and load variables (x- and z-displacement profiles, maximum x- and z-displacements, timing of these motion vectors, upper and lower neck axial and shear forces and sagittal bending moments), as illustrated in the respective figures, it can be concluded that the repeatability performance of the THOR dummy is acceptable at all velocities. This type of evaluation using many variables adds confidence to the use and evaluation of this dummy for a range of external frontal impact insults.

In order to evaluate the biofidelity of any advanced frontal dummy such as the THOR, it is important to match the PMHS corridors under simulated impacts, sled experiments for example. Peak responses such as forces and

moments at the ends of the neck as a function of velocity on a component level can be compared with corresponding PMHS data expressed as mean, plus/minus one standard deviation, serving as corridors. While this process compares maximum metrics, time-dependent behaviors can be evaluated by overlaying dummy responses (example force histories) on PMHS corridors. While this process can be used on a component level such as those used in the present study for the head-neck system, another methodology would be to evaluate the biofidelity of the entire dummy. This may be done by grouping individual component responses and using quantitative methods such as a ranking system with component-specific or loading-specific weighting scheme. The present head-neck results can be used in such a process. Studies evaluating entire dummy biofidelity are considered to be future research wherein responses should be combined from other regions such as the thorax and pelvis.

The mass-less neck assumption used to derive PMHS lower neck loads simplified the computation process by eliminating the influence of the kinematics of the neck complex consisting of the osteo-ligamentous column with the surrounding passive musculature on derived metrics. Because of the low but finite mass of the neck complex compared to the head, its motions affect lower neck forces and moments. As different PMHS have different neck compliances and mass, relative magnitudes of the effects of the mass-less neck assumption are specimen dependent and unknown. From this perspective, the present results should be considered as a first step in the understanding and quantification of lower neck injury biomechanical metrics. Comparison of computed lower neck loads using head acceleration data and mass-less neck assumption to measured lower neck loads in dummy tests while appear reasonable, they are not precise to evaluate the accuracy of the assumption in PMHS. This is because of the coupling and compliance differences between the two types of surrogates, example PMHS and THOR. In order to determine the accuracy of the assumption in PMHS tests, it would be necessary to develop detailed and accurate finite element models. Using fully verified and validated models, it would be possible to assess the accuracy of the mass-less neck assumption. Ongoing efforts by the Global Human Body Model Consortium may offer an opportunity to investigate these issues, and results from the present study can be used by finite element modelers in the future.

It is known that the PMHS model incorporates only passive musculature. Lack of active-resting muscle tone does not replicate in vivo situations. From this perspective, this is a limitation of any PMHS model. However, the pretest alignment of the head-neck system used in the present study was such that the Frankfurt plane was horizontal and the cervical spinal column was in its “natural” lordotic posture. These processes approximated in vivo situations as closely as possible in the intact PMHS.

It should be noted that human volunteer and PMHS experimental data were used during the development of the THOR. For example, frontal impact human volunteer data from the Naval Biodynamics Laboratory in New Orleans, USA was used. These data were obtained from sled tests using young human subjects albeit with differing restraint systems. Likewise, PMHS data in the axial mode reflecting improved compliance compared to its predecessor were also used during the neck design of the THOR which eventually resulted in anterior and posterior cables representing the different load paths separating osteo-ligamentous column and neck (including muscle) loads. These considerations may be responsible for the good correlation in head-neck kinematics and upper and lower neck loads at different velocities, as demonstrated by the results of the present study. From these perspectives also, this device appears to be an improved dummy for frontal impacts in motor vehicle environments.

Regarding forces and moments at the upper and lower necks, the presence of two load cells in the dummy and the use of appropriate instrumentation in PMHS tests made it possible to evaluate its biofidelity performance from the load absorption/transmission perspective, described earlier [6-8]. Injuries to the upper neck are best described by metrics associated with the rostral region. Likewise, traumas to the lower regions are best addressed by the associated caudal metrics. As the caudal end of the neck is often involved in trauma to survivors, forces and moments obtained from the lower neck load cell representing the cervico-thoracic junction in the human may be used in crashworthiness evaluations [10-14].

Axial and shear forces and moments occur in the neck due to the kinematics and coupling between the neck and head in frontal impacts in any surrogate. In the *in vivo* human, occipital condyles act as the osteo-ligamentous connectivity between the base of the skull and cervical spine for axial load and bending moment transmissions; and facet joints in the column also serve as a secondary load path for the transmission of the external loading [15]. Although muscles stabilize the ligamentous column by controlling the pre-alignment of the neck with respect to the head, the initial posture of the neck cannot be altered by the activation of muscles as the time response during the loading process is short [16-18]. In the THOR, the kinematics and coupling occurs through the combination of rubber pucks interconnected by metallic discs and cables [3].

Judging by similarities in curve morphologies in both tested surrogates, it can be concluded that the THOR mimics the human responses well at both ends of the head-neck complex and at all velocities. Furthermore, these results suggest that the THOR can be used effectively in frontal impact crashworthiness tests regardless of the change in velocity. This is primarily true for the head-neck response, the topic of this paper. It should be noted that the current presentation confined to the THOR evaluation. As indicated in the introductory paragraphs, the Hybrid III dummy was developed using data available to researchers and dummy designers during the 1970s. In contrast, more recent biomechanical data were available to design the THOR as it was envisaged in the 1990s. This later dummy has the ability to differentiate between cervical column and neck loads and is more complaint in the axial mode, also stated earlier. As data from the United States National Automotive Sampling System (NASS) have begun to show injuries and importance of testing at lower speeds, results from the present investigation indicating that the THOR may be the most suitable test device adds confidence in using this model for future crashworthiness analyses. Additional tests including full-scale and sled experiments are be needed to reinforce these observations.

V. ACKNOWLEDGEMENTS

This research study was supported in part by DTNH22-07-H00173 and VA Medical Research. The authors of the study thank Drs. Rodney Rudd and Stephen Ridella of NHTSA for their technical assistance.

VI. REFERENCES

[1] Kuppa, S., Eppinger, R. H., McKoy, F., Nguyen, T., Pintar, F. A., and Yoganandan, N., "Development of side impact thoracic injury criteria and their application to the modified ES-2 dummy with rib extensions (ES-2re)," Stapp Car Crash J, 47, pp. 189-210,2003.

[2] Yoganandan, N., Sances, A., Jr., and Pintar, F., "Biomechanical evaluation of the axial compressive responses of the human cadaveric and manikin necks," J Biomech Eng, 111(3), pp. 250-255,1989.

[3] Rangarajan, N., White, A., Shams, T., Beach, D., Fullerton, J., Haffner, M., Eppinger, R. H., and Pritz, H., "Design and performance of the THOR advanced frontal crash test dummy " 16th International Conference on Enhanced Safety of Vehicles Windsor, Canada, pp. 1999-2010, 1996.

[4] White, R., Zhao, Y., Rangarajan, N., Haffner, M., and Epinger, R., "Development of an instrumented biofidelic neck for the advanced frontal test dummy," 15th International Conference on Enhanced Safety of VehiclesMelbourne,m Australia, pp. 1728-1741, 1996.

[5] SAE, "Society of Automotive Engineers," Instrumentation for impact test-Part 1-electonic Instrumentation-SAE J211/1Warrendale, PA, 1995.

[6] Pintar, F. A., Yoganandan, N., and Maiman, D. J., "Lower cervical spine loading in frontal sled tests using inverse dynamics: potential applications for lower neck injury criteria," Stapp Car Crash J, 54, pp. 133-166,2010.

[7] Yoganandan, N., Zhang, J., Pintar, F. A., and King Liu, Y., "Lightweight low-profile nine-accelerometer package to obtain head angular accelerations in short-duration impacts," J Biomech, 39(7), pp. 1347-1354,2006.

[8] Yoganandan, N., Maiman, D. J., Guan, Y., and Pintar, F., "Importance of physical properties of the human head on head-neck injury metrics," Traffic Inj Prev, 10(5), pp. 488-496,2009.

[9] Yoganandan, N., Pintar, F. A., Maiman, D. J., Philippens, M., and Wismans, J., "Neck forces and moments and head accelerations in side impact," Traffic Inj Prev, 10(1), pp. 51-57,2009.

[10] Claytor, B., MacLennan, P. A., McGwin, G., Jr., Rue, L. W., 3rd, and Kirkpatrick, J. S., "Cervical spine injury

and restraint system use in motor vehicle collisions," Spine (Phila Pa 1976), 29(4), pp. 386-389; discussion Z382,2004.

[11] Wang, M. C., Pintar, F., Yoganandan, N., and Maiman, D. J., "The continued burden of spine fractures after motor vehicle crashes," J Neurosurg Spine, 10(2), pp. 86-92,2009.

[12] Yoganandan, N., Haffner, M., Maiman, D. J., Nichols, H., Pintar, F. A., Jentzen, J., Weinshel, S., Larson, S. J., and Sances, A., Jr, "Epidemiology and injury biomechanics of motor vehicle related trauma to the human spine," SAE Transactions, 98(6), pp. 1790-1807,1990.

[13] Pintar, F. A., Yoganandan, N., and Maiman, D. J., "Injury mechanisms and severity in narrow offset frontal impacts," Ann Adv Automot Med, 52, pp. 185-189,2008.

[14] Yoganandan, N., Pintar, F. A., Stemper, B. D., Schlick, M., Philippens, M., and Wismans, J., "Biomechanics of human occupants in simulated rear crashes: documentation of neck injuries and comparison of injury criteria," Stapp Car Crash J, 44, pp. 189-204,2000.

[15] Yoganandan, N., Pintar, F. A., Larson, S. J., and Sances, A., Jr, eds., Frontiers in Head and Neck Trauma: Clinical and Biomechanical, 743 pp,IOS Press, The Netherlands, 1998.

[16] Stemper, B. D., Yoganandan, N., Rao, R. D., and Pintar, F. A., "Reflex muscle contraction in the unaware occupant in whiplash injury," Spine (Phila Pa 1976), 30(24), pp. 2794-2798; discussion 2799,2005.

[17] Yoganandan, N., Pintar, F. A., and Kleinberger, M., "Whiplash injury. Biomechanical experimentation," Spine (Phila Pa 1976), 24(1), pp. 83-85,1999.

[18] Maiman, D. J., Yoganandan, N., and Pintar, F. A., "Preinjury cervical alignment affecting spinal trauma," J Neurosurg, 97(1 Suppl), pp. 57-62,2002.